Available online at www.sciencedirect.com
ScienceDirect
Journal of Power Sources 164 (2007) 874–879
JOURNAL OF POWER SOURCES
www.elsevier.com/locate/jpowsour

Short communication

Fabrication and electrochemical properties of three-dimensional net architectures of anatase TiO_2 and spinel $Li_4Ti_5O_{12}$ nanofibers

Hai-Wei Lu, Wei Zeng, Yue-Sheng Li, Zheng-Wen Fu *

Department of Chemistry & Laser Chemistry Institute, Department of Material Science, Shanghai Key Laboratory of Molecular Catalysts and Innovative materials, Fudan University, Shanghai 200433, PR China

Received 9 September 2006; received in revised form 1 November 2006; accepted 2 November 2006
Available online 5 December 2006

Abstract

As a new type of electrodes engineering method with three-dimensional (3D) architecture for 3D rechargeable lithium ion batteries, an electrospinning has been successfully employed to prepare 3D net architectures of anatase TiO_2 and spinel $Li_4Ti_5O_{12}$ nanofibers. Scanning electron microscopy, X-ray diffraction, cyclic voltammetry and the discharge/charge measurements were used to characterize their structures and electrochemical properties. Our results demonstrated that 3D architectures stacked from a cross-bar array of electrospun anatase TiO_2 nanofibers could be accomplished but were destroyed after the insertion of Li ion. Significantly, spinel $Li_4Ti_5O_{12}$ could be selected as one of promise candidates for the realization of 3D batteries considering its structure stability of 3D spinel $Li_4Ti_5O_{12}$ nanofibers associated with well cyclability.

Keywords: Electrospinning; Three-dimensional rechargeable lithium ion batteries; Nanofibers; TiO_2; $Li_4Ti_5O_{12}$

1. Introduction

An extensive research effort is currently underway to produce three-dimensional (3D) battery architectures for rechargeable lithium ion batteries due to the increase of the containing areas between the cathode and anode electrodes, which could provide a way to maximize energy and power density [1,2]. Various approaches have been reported for introducing 3D electrode structures within battery by micromachining [3,4] or templating [5–7]. For example, Wang et al. microfabricated high aspect ratio carbon posts by pyrolyzing SU-8 negative photoresist, in which photolithography can be used to pattern electrode arrays [3]. Lytle et al. reported the synthesis and electrochemical properties of 3D ordered macroporous SnO_2 electrode, in which close-packed arrays of uniform spheres were used as templates, and appropriate precursors infiltrated them, and then these composites were processed to remove the template and to form solid wall skeletons [5]. It was found that 3D electrodes presented high accessible surface areas, continuous networks and structure features for the design of novel battery. New strategies designed around electrodes engineered with 3D architecture are still being developed. Recently, Li et al. made a mighty advance in electrospinning technique for uniaxially aligned arrays of ceramic nanofibers by the use of a collector consisting of a gap between two conductive substrates [8–11]. If controlling the configuration of the collector, the uniaxially aligned arrays of nanofibers could be stacked in a cross-bar and a layer-by-layer fashion to generate a 3D net structure. Enlightened by their works [10,11], 3D net architectures of electrode can be readily prepared by electrospinning for further investigating the electrochemical properties of 3D battery. Here, we demonstrate that 3D net architectures of anatase TiO_2 and spinel $Li_4Ti_5O_{12}$ nanofibers can be conveniently prepared by electrospinning. One of the attractive features associated with this method is a simple and versatile for generating fibers from a rich variety of materials as cathodic or anodic electrodes for Li ion batteries.

More efforts must be made to investigate the electrochemical characteristics of 3D structure electrode for the realization of 3D batteries. As typical cathode materials used in rechargeable lithium batteries, TiO_2 and $Li_4Ti_5O_{12}$ were promising storage lithium materials [12–17]. Recently, we reported electrochemical characterization of 3D ordered macroporous (3DOM) anatase TiO_2 electrode by a colloidal crystal templating approach combining with a high temperature calci-

* Corresponding author. Tel.: +86 21 65642522; fax: +86 21 65102777.
E-mail address: zhengwen@sh163.net (Z.-W. Fu).

0378-7753/$ – see front matter © 2006 Elsevier B.V. All rights reserved.
doi:10.1016/j.jpowsour.2006.11.009

nating, and found the destruction of 3DOM TiO_2 film when Li ions are inserted into TiO_2, indicating that it is rather difficult to realize 3D batteries with using 3DOM anatase TiO_2 electrodes [12]. In order to further evaluate this conclusion, we try to reinvestigate the electrochemical characteristics of 3D anatase TiO_2 electrode by new 3D net structure with features of bar. In addition, 3D net architectures of spinel $Li_4Ti_5O_{12}$ was prepared firstly and its electrochemical behavior was examined to clarify the nature of electrochemical properties of 3D batteries.

2. Experiment

An electrospinning setup for the fabrication of fibers included a syringe pump (KDS-200, Stoelting Co., Wood Dale, IL), a collector electrode, a plastic syringe equipped with a N6 gauge needle made of stainless steel with the inner and outer diameters of 0.6 and 0.8 mm, respectively, and a dc voltage generator (up to 20 kV). A dc voltage about 1.2 kV was applied between the outside of a N6 gauge needle and a collector electrode. The stainless steel was used as the collector electrode. The distance between a collector and the tip of the needle was ~20 cm. A syringe pump was employed to control the feeding rate of 0.5 ml h^{-1} for the precursor solution. The electrospinning process was conducted in air. The collector contained a gap in the middle of two gold electrodes. The width of the gap is about 1 cm. The electric field lines in the vicinity of the collector were split into two fractions pointing toward opposite edges of the gap, so aligned nanofibers which paralleled in long axis can be achieved [10,11].

One milliliter of titanium tetraisopropoxide ($Ti(OiPr)_4$, Aldrich) was mixed with 7 ml of isopropyl alcohol in a glovebox. After stirring for ~10 min, 0.3 g of PVP (Aldrich, M_w = 1,300,000) was added to this solution. The mixture was immediately loaded into a plastic syringe after magnetic stirring ~1 h and was used as an electrospinning precursor solution for the fabrication of TiO_2 fibers. The as-spun nanofibers were left in air for ~5 h to allow the hydrolysis of $Ti(OiPr)_4$ to go to completion. Finally, PVP was selectively removed from these nanofibers by treating them in air at 500 °C for 1 h. In addition, Li-Ti-O/PVP sol with the stoichiometric ratio of Li:Ti:PVP = 4:5:4 sol for the fabrication of $Li_4Ti_5O_{12}$ fibers was also prepared by the similar routine, in which 0.18 g lithium acetylacetonate ($Li(CH_3COCHCOCH_3)$, Aldrich) was dissolved in a solvent mixture of a precursor solution for TiO_2 fibers mentioned above. PVP in $Li_4Ti_5O_{12}$/PVP fibers was removed after calcining in air at 750 °C.

X-ray diffraction (XRD) patterns and the morphology of 3D electrodes were recorded by a Rigata/max-C diffractometer with Cu Kα radiation and scanning electron microscopy (SEM) (Pillips XL-30), respectively. Weights of 3D TiO_2 or $Li_4Ti_5O_{12}$ was directly obtained by subtracting the original substrate weight from total weight of the substrate and the deposited 3D film onto its surface, which were examined by electrobalance (BP 211D, Sartorius).

For the electrochemical measurements, the two or three electrode cells were constructed by using 3D electrode as a working electrode and one or two lithium sheets as a counter electrode and a reference electrode, respectively. 3D net architectures of anatase TiO_2 and spinel $Li_4Ti_5O_{12}$ nanofibers deposited on the stainless steel substrate by electrospinning were directly used as a working electrode without any other binder or conductive agents. The electrolyte consisted of 1 M $LiPF_6$ in a nonaqueous solution of ethylene carbonate (EC) and dimethyl carbonate (DMC) with a volume ratio of 1:1 (Merck). The cells were assembled in an Ar filled glove box. The two-electrode cell was used for discharge/charge measurement, which was performed at room temperature with a Land BT 1–40 battery test system. The cell was cycled between 1.0 and 3.5 V versus Li/Li^+. The three-electrode cell was used for cycle voltammogram measurement, which was carried out with a CHI 660a electrochemical working station (CHI Instruments).

3. Result and discussion

In order to prepare uniform nanofibers in diameters, it is necessary to control the electrospinning conditions, such as PVP concentration, $Ti(OiPr)_4$ concentrations, the feeding rate and the strength of electric field. Under our experimental conditions, the diameter of TiO_2/PVP nanofibers of 350 ± 20 nm could be prepared as uniaxially aligned arrays. As Fig. 1(a), a parallel array of TiO_2/PVP nanofibers was electrospun from the precursor solution of $Ti(OiPr)_4$ for 60 s. We made some progress on the collectors, so the collector could be rotated by any angle. By rotating the collector by 90°, the another layer fibers with its long axes perpendicular to the first layer was stacked together as shown in Fig. 1(b). By using this method, a 3D TiO_2/PVP nanofibers network structure can be made. The density of the nanofibers can be controlled by collecting time, and the number of layer of the network structure is determined by the rotating number of the collector. In fact, the formation of 3D nanofibers network is a complicated process, the feature of nanofibers and the electrical field parameters can influence its formation. The fiber suspended across the gap can remain highly charged after deposition, thus the electrostatic repulsion between the deposited and the upcoming fibers can further enhance the parallel alignment. But if there is a tiny disturb of the electrical field, the fibers will be entwisted together as shown in Fig. 1(c). So it is often difficult to get large density of paralleled nanofibers with long collection time.

Properly adjusting the pH of the precursor solution (slightly decline the resistance) for electrospinning, it can decrease the electrostatic effect between the fibers after deposition, so as to avoid the fibers to be twisted. In our experiment, we added one or two drops of acetic acid into the precursor solution. The deposited fibers were well aligned and could be stacked in multilayer with their long axes perpendicular to each others as shown in Fig. 1(d), even when the collecting time was very long for 1 h. Fig. 1(e) shows SEM image of 3D network architecture after annealed in air at 500 °C for 1 h to remove PVP. The mean diameter of nanofibers declined to 250 ± 20 nm. High temperature annealing will cause the stress of the network structure. Some of the nanofibers were bent. In order to release the stress, the annealing temperature raised slowly from the room temperature to 500 °C for 5 h. When the typical 3D network architecture

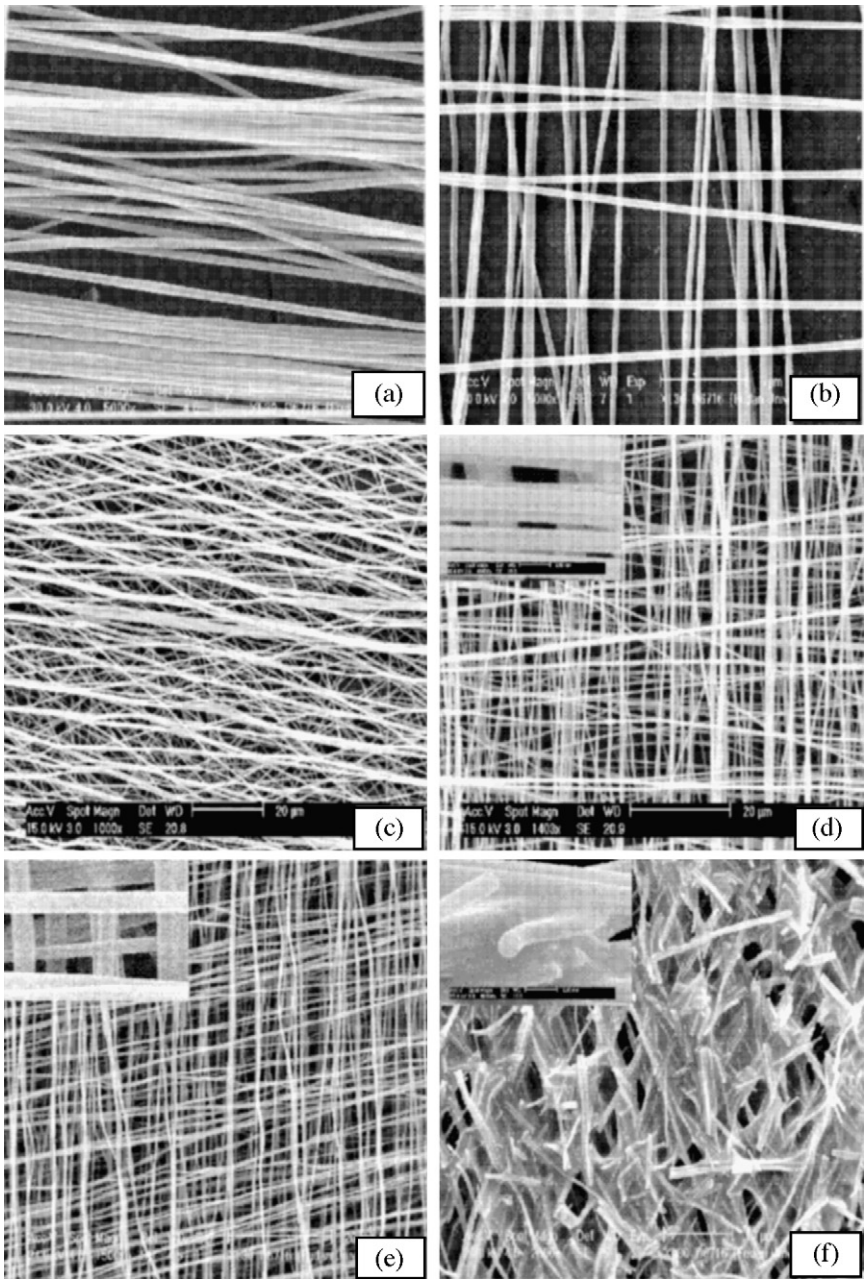

Fig. 1. SEM micrographs of uniaxially aligned TiO_2/PVP nanofibers arrays. (a) Monolayer; (b) two perpendicular layers; (c) and (d) multilayer nanofibers without and with the addition of acetic acid in precursor solution; (e) nanofibers network structure after annealed at 500 °C; (f) after electrochemical reaction. The insets show enlarged SEM images of these nanofibers.

as cathode was assembled with lithium into the cell, SEM of its surface images after the first electrochemical reaction of 3D architecture with Li was shown in Fig. 1(f). A majority of fibers from surface to more layers were interrupted, and the overall 3D net architecture has been destroyed after lithium inserted.

Anatase TiO_2 nanofibers with the 3D network structure was well preserved after annealed at high temperature, which can be examined by XRD and CV data as shown in Fig. 2(a and b), respectively. Fig. 2(a) shows XRD pattern of 3D TiO_2 nanofibers network annealed at 500 °C and after inserted by lithium. Apart from diffraction peaks appearing at $2\theta = 43.6^\circ$ and 50.7°, which can be attributed to the stainless steel substrate, the annealed 3D TiO_2 nanofibers exhibited a clear diffraction peak at 25.3°, which can be indexed to (1 0 1) reflection peak of the anatase TiO_2 (PDF#89-4921). After lithium insertion reaction to 1.0 V in 3D TiO_2/Li cells, the diffraction peak of (1 0 1) anatase TiO_2 disappear in XRD pattern, implying that the crystalline structure of 3D TiO_2 nanofibers network is different form anatase, and is amorphous or the particles size of nano-crystalline formed after lithium insertion into 3D TiO_2 nanofibers is less than the wavelength of coherent X-ray.

As shown in Fig. 2(b), a couple of peaks were observed at 1.18 and 2.33 V versus Li/Li^+ at the scan rate of 0.001 V s^{-1}, exhibiting a typical feature of TiO_2 electrode [12,13]. They cor-

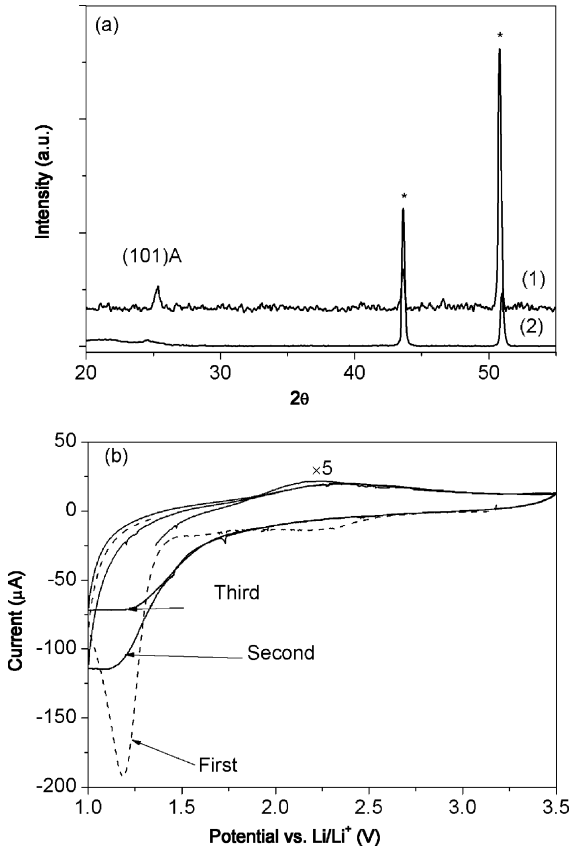

Fig. 2. (a) XRD patterns of annealed TiO_2 3D nanofibers arrays (1) before and (2) after electrochemical reaction, the peaks marked with an asterisk correspond to stainless steel substrate; (b) cyclic voltammogram curves of 3D anatase TiO_2/Li cell.

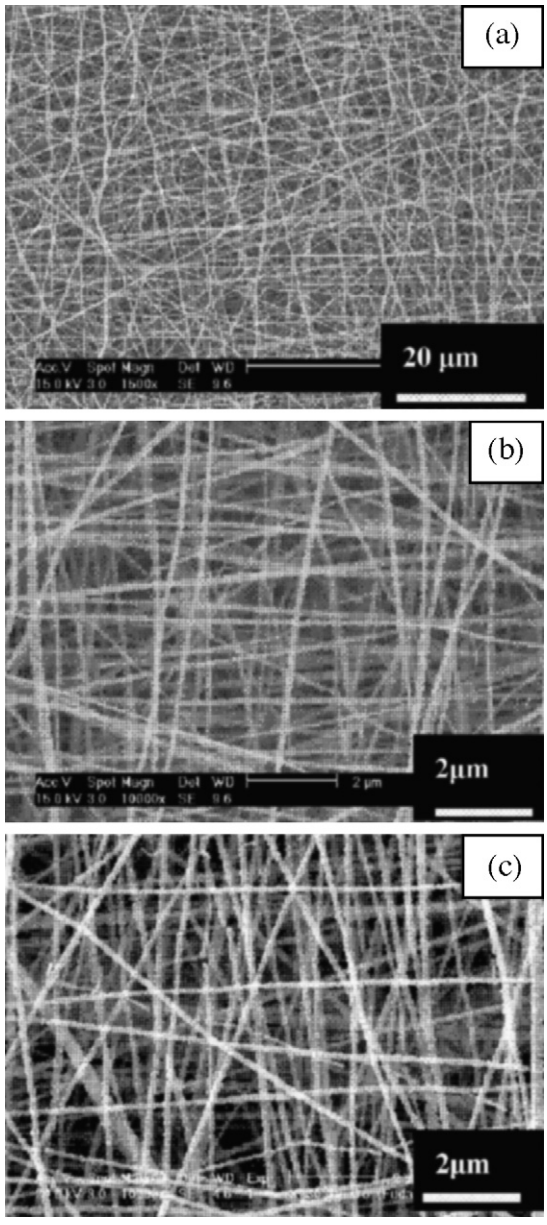

Fig. 3. SEM images of $Li_4Ti_5O_{12}$/PVP fibers before (a) and (b) after calcining in air 750 °C for 1 h fabricated by electrospinning, (c) SEM images of $Li_4Ti_5O_{12}$ fibers after electrochemical reaction.

responded to the insertion and the extraction processes of Li for 3D TiO_2. The fade of the curves between the first and subsequent cycles shows the large irreversible process after the insertion of Li into TiO_2 anatase structure. Combined with SEM and XRD data mentioned above, the destruction of 3D architecture and anatase structure of TiO_2 nanofibers when Li ions are inserted into TiO_2 should be responsible for capacity fades during the cycles. These results were consistent with previous investigation [12]. Previous studies indicated that lithium insertion in anatase TiO_2 could causes the volume expansion of 3% due to the increase of lithium titanate phase [14]. The continuous enlargement of the volumes after Li insertion into TiO_2 may result in mechanical destruction of 3D architecture.

Apparently, the structure and mechanical stability should be considered when selecting electrode materials for 3D architecture. Spinel $Li_4Ti_5O_{12}$ has been demonstrated as zero-strain lithium insertion hosts in the discharge/charge process [15–17]. An attempt using $Li_4Ti_5O_{12}$ instead of TiO_2 nanofiber for 3D architecture was made. Fig. 3(a) shows SEM images of collected fibers by electrospinning an ethanol solution containing 0.27 M PVP and 0.27 M $Li_4Ti_5O_{12}$. These fibers were randomly distributed on the substrate and their lengths could reach several micrometers. The mean diameter of these fibers was found to be 280 ± 50 nm. These fibers may consist of PVP and $Li_4Ti_5O_{12}$. After burning the sample in air at 750 °C, the PVP was removed, a well-defined fiber texture kept unchangeable. As shown in Fig. 3(b), their mean diameter was found to be 150 ± 50 nm. These fibers were composed of very small crystalline grains uniformly linked with an average size less than 100 nm, indicating the nanostructure of the fibers. Interestingly, after electrochemical reaction of these $Li_4Ti_5O_{12}$ nanofibers with Li, the nanofibers structure kept constant as shown in Fig. 3(c). This is utterly different from the case of TiO_2 fibers. The size reduction of the fibers after burning could be due to the loss of PVP from the fibers and the crystallization, which could be confirmed by XRD measurement.

Fig. 4(a) shows XRD patterns of the phase obtained before and after chemical insertion of Li. All of observed diffraction peaks can be indexed in the Fd3m space group of the cubic spinel

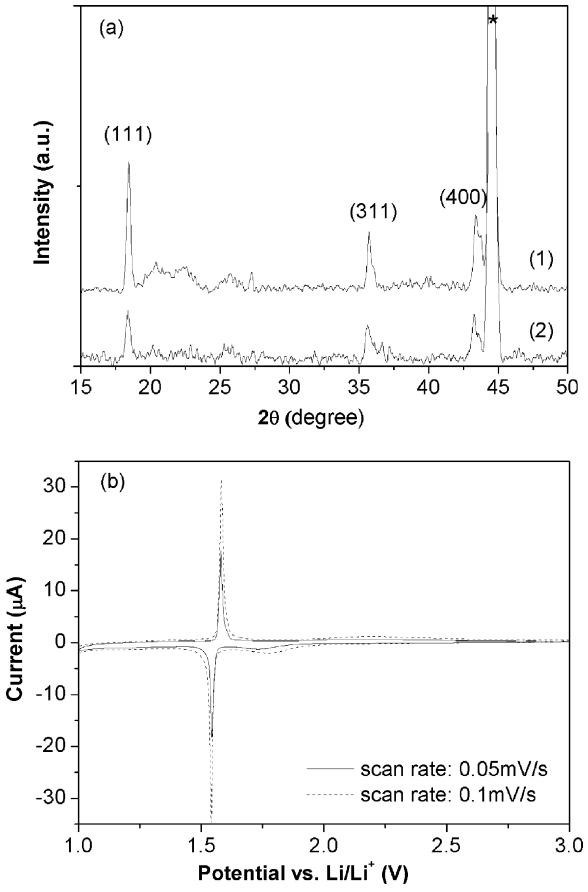

Fig. 4. (a) XRD patterns of annealed $Li_4Ti_5O_{12}$ nanofibers arrays (1) before and (2) after electrochemical reaction, the peaks marked with an asterisk correspond to stainless steel substrate; (b) cyclic voltammogram curves of spinel $Li_4Ti_5O_{12}$ fibers/Li cell at the different scan rates.

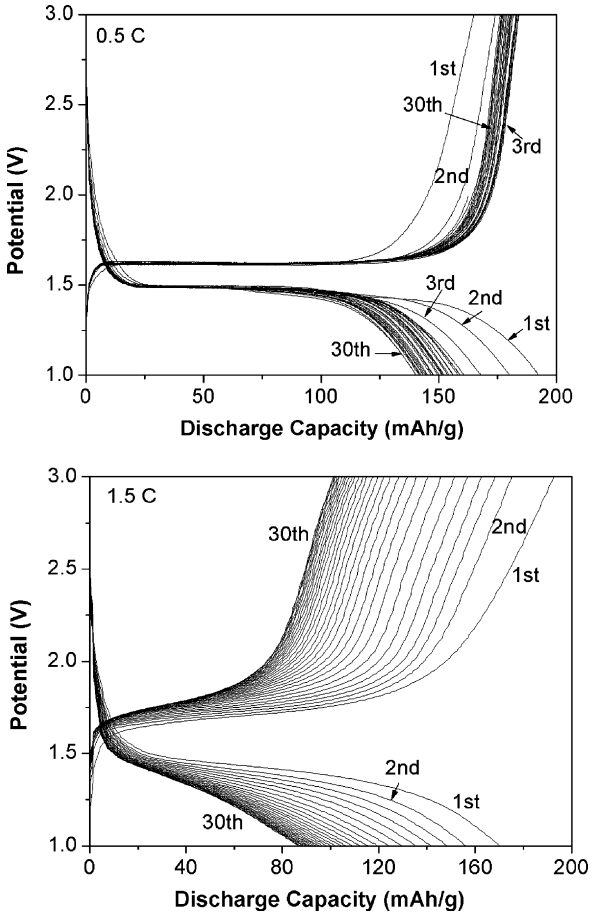

Fig. 5. Voltage profile of 3D spinel $Li_4Ti_5O_{12}$ nanofibers/Li cell at the discharge/charge rates of 0.5*C* and 1.5*C*.

structure, which is in agreement with previous report [18]. Apart from slight variations in relative peak intensities between before and after chemical insertion of Li, there were the same diffraction peaks in both XRD patterns, indicating that spinel $Li_4Ti_5O_{12}$ can keep structure stability during electrochemical cycling, in which lithium ions are located at the tetrahedral 8(a) sites and tetravalent titanium ions and lithium ions are randomly distributed at octahedral 16(d) sites, while oxygen ions are located at the 32(e) sites. As a result, 3D spinel $Li_4Ti_5O_{12}$ nanofibers exhibit well reversibility during the insertion and extraction of Li as shown in Fig. 4(b). The lithium insertion and extraction peaks at 1.54 and 1.58 V versus Li/Li^+ were both reversible in a typical cyclic voltammogram of 3D spinel $Li_4Ti_5O_{12}$ nanofibers/Li cell.

The voltage profiles of 3D spinel $Li_4Ti_5O_{12}$ nanofibers at different discharge/charge rates are shown in Fig. 5. This voltage profile was a typical behavior of spinel $Li_4Ti_5O_{12}$. The first five discharge capacities were 140–192 mAh g^{-1} at 0.5*C* with a capacity loss of 1.0% per cycle. When the discharge rate increased to 1.5*C*, the discharge capacities ranged in 87–170 mAh g^{-1} in the first 30 cycles with a capacity loss of 1.6% per cycle. Apparently, the discharge capacity of $Li_4Ti_5O_{12}$ nanofibers decreased rapidly at 1.5*C* rate, while its stability was excellent at 0.5*C* rate. These results showed that the insertion and extraction processes were stable and reversible, which should be related to the structure stability of 3D spinel $Li_4Ti_5O_{12}$ nanofibers confirmed by SEM and XRD. The 3D architecture may mitigate the influence of slow lithium ion diffusivity in solid bulk and improve the rate capability of lithium insertion.

4. Conclusion

In this study, 3D network architecture of anatase TiO_2 and spinel $Li_4Ti_5O_{12}$ have been prepared by electrospinning and their electrochemical properties as cathode materials for 3D rechargeable Li ion batteries have been examined by CV and discharge/charge measurements. After Li ions insertion, the destruction of 3D network architectures of TiO_2 nanofibers associated with poor cycle performance was found, while $Li_4Ti_5O_{12}$ exhibited a stable in 3D network architectures and good reversible in electrochemical cycles. $Li_4Ti_5O_{12}$ can be expected to have potential application for 3D batteries as a zero-strain insertion material. It should be emphasized that a simple and versatile method based on electrospinning for preparing uniaxially aligned nanofibers could be extended to other electrode materials of storage energy such as $LiCoO_2$, $LiMn_2O_4$, $LiFePO_4$, SnO for the application of 3D batteries.

Acknowledgement

This work was supported by the National Nature Science Foundation of China (Project No. 20203006).

References

[1] J.W. Long, B. Dunn, D.R. Rolison, H.S. White, Chem. Rev. 104 (2004) 4463.
[2] R.W. Hart, H.S. White, B. Dunn, D.R. Rolison, Electrochem. Commun. 5 (2003) 120.
[3] C. Wang, L. Taherabadi, G. Jia, M. Madou, Y. Yeh, B. Dunn, Electrochem. Solid-State Lett. 7 (2004) A435.
[4] G. Baure, C.W. Kown, G.G. Lee, F. Chamran, C.J. Kim, B. Dunn, in: E.J. Barandon, A. Ryan, J. Harb, R. Ulrich (Eds.), Micropower and Microdevices, vol. PV2002-25, The Electrochemical Society Proceedings Series, Pennington, NJ, 2003.
[5] O.J.C. Lytle, H. Yan, N.S. Ergang, W.H. Smyrl, A. Stein, J. Mater. Chem. 14 (2004) 1616.
[6] A. Stein, R.C. Schroden, Curr. Opin. Solid State Mater. Sci. 5 (2001) 553.
[7] H. Yan, S. Sokolov, J.C. Lytle, A. Stein, F. Zhang, W.H. Smyrl, J. Electrochem. Soc. 150 (2003) A1102.
[8] D. Li, Y. Xia, Nano Lett. 3 (2003) 555.
[9] D. Li, G. Ouyang, J.T. McCann, Y. Xia, Nano Lett. 5 (2005) 913.
[10] D. Li, Y. Wang, Y. Xia, Nano Lett. 3 (2003) 1167.
[11] D. Li, Y. Xia, Adv. Mater. 16 (2004) 1151.
[12] B. Zhang, Y. Yuan, Y. Wang, Z.W. Fu, Electrochem. Solid-State Lett. 9 (2006) A101.
[13] Z.W. Fu, J.L. Kong, Q.Z. Qin, Z.Q. Tian, Sci. China (Ser. B) 42 (1999) 493.
[14] M. Wagemaker, G.J. Kearley, A.A. van Well, H. Mutka, F.M. Mulder, J. Am. Chem. Soc. 125 (2003) 840.
[15] K. Zaghib, M. Armand, M. Gauthier, J. Electrochem. Soc. 145 (1998) 3135.
[16] S. Panero, D. Staolli, M. Salomon, B. Scrosati, Electrochem. Commun. 2 (2000) 810.
[17] K. Nakahara, R. Nakajima, T. Matsushima, H. Majima, J. Power Sources 17 (2003) 131.
[18] A. Deschanvres, B. Raveau, Z. Sekkal, Mater. Res. Bull. 6 (1971) 699.